Journal of Structural Biology 205 (2019) 189–195

Contents lists available at ScienceDirect

Journal of Structural Biology

journal homepage: www.elsevier.com/locate/yjsbi

Structural transformation-mediated dimerization of caspase recruitment domain revealed by the crystal structure of CARD-only protein in frog virus 3

Chang Min Kim[a,1], Hyun Ji Ha[a,1], Sunghark Kwon[a,1], Jae-Hee Jeong[b], Sung Hoon Lee[c], Yeon-Gil Kim[b], Chang Sup Lee[d], Jun Hyuck Lee[e], Hyun Ho Park[a,*]

[a] College of Pharmacy, Chung-Ang University, Seoul 06974, Republic of Korea
[b] Pohang Accelerator Laboratory, Pohang University of Science and Technology, Pohang 790-784, Republic of Korea
[c] Department of Pharmacology, College of Pharmacy, Chung-Ang University, Seoul 06974, Republic of Korea
[d] College of Pharmacy and Research Institute of Pharmaceutical Sciences, Gyeongsang National University, Jinju 52828, Republic of Korea
[e] Unit of Polar Genomics, Korea Polar Research Institute, Incheon 21990, Republic of Korea

ARTICLE INFO

Keywords:
Apoptosis
Death domain superfamily
Caspase recruitment domain
CARD-only protein
Crystal structure
Domain swapping

ABSTRACT

Caspase recruitment domain (CARD)-only proteins (COPs), regulate apoptosis, inflammation, and innate immunity. They inhibit the assembly of NOD-like receptor complexes such as the inflammasome and NODosome, which are molecular complexes critical for caspase-1 activation. COPs are known to interact with either caspase-1 CARD or RIP2 CARD via a CARD-CARD interaction, and inhibit caspase-1 activation or further downstream signaling. In addition to the human COPs, Pseudo-ICE, INCA, and ICEBERG, several viruses also contain viral COPs that help them escape the host immune system. To elucidate the molecular mechanism of host immunity inhibition by viral COPs, we solved the structure of a viral COP for the first time. Our structure showed that viral COP forms a structural transformation-mediated dimer, which is unique and has not been reported in any structural study of a CARD domain. Based on the current structure, and the previously solved structures of other death domain superfamily members, we propose that structural transformation-mediated dimerization might be a new strategy for dimer assembly in the death domain superfamily.

1. Introduction

The caspase recruitment domain (CARD) is protein-protein interaction module that belongs to the death domain superfamily (DDS), which is considered to be the largest class of protein interaction modules (Park et al., 2007). DDS-containing proteins play a pivotal role in apoptosis, inflammation, necrosis, and immune cell signaling pathways (Park et al., 2007; Kwon et al., 2012). The assembly of caspase-activating complexes, such as the apoptosome (Acehan et al., 2002), the PIDDosome (Park et al., 2007), the death-inducing signaling complex (DISC) (Dickens et al., 2012), and the inflammasome (Lu et al., 2014; Hornung et al., 2009), occurs via homo- and hetero-oligomeric DDS interactions. Additionally, DDS also mediates the recruitment of downstream effectors for immune cell receptor signaling and intracellular pathogen sensing (Stanger et al., 1995; Golstein et al., 1995; Akira et al., 2006; Pichlmair et al., 2006).

The DDS is comprised of four subfamilies. In addition to the CARD subfamily, the other DDS subfamilies are the death domain (DD) family, the death effector domain (DED), and the PYrin domain (PYD). Classification of subfamilies within the superfamily is mainly by sequence homology and unique structural characteristics (Park et al., 2007; Kwon et al., 2012). Although the six-helical bundle structural fold is a well-known unifying feature of the DDS, several unique features in each subfamily, such as a more flexible and exposed third helix in the DDs, the presence of an RxDL-motif in the DEDs, an interrupted, bent first helix in the CARDs, and a relatively small or disrupted third helix in the PYDs, have been identified through structural studies (Park et al., 2007; Sukits et al., 2001; Tsao et al., 2000; Yang et al., 2005; Bae and Park, 2011; Hofmann et al., 1997). In the human genome, 37 proteins with DDs, 7 proteins with DEDs, 33 proteins with CARDs, and 22 proteins with PYDs have been identified.

PYD-only proteins (POPs) and CARD-only proteins (COPs) have

* Corresponding author.
E-mail address: xrayleox@cau.ac.kr (H.H. Park).
[1] These authors contributed equally to this work.

https://doi.org/10.1016/j.jsb.2018.12.006
Received 16 September 2018; Received in revised form 19 December 2018; Accepted 22 December 2018
Available online 06 January 2019
1047-8477/

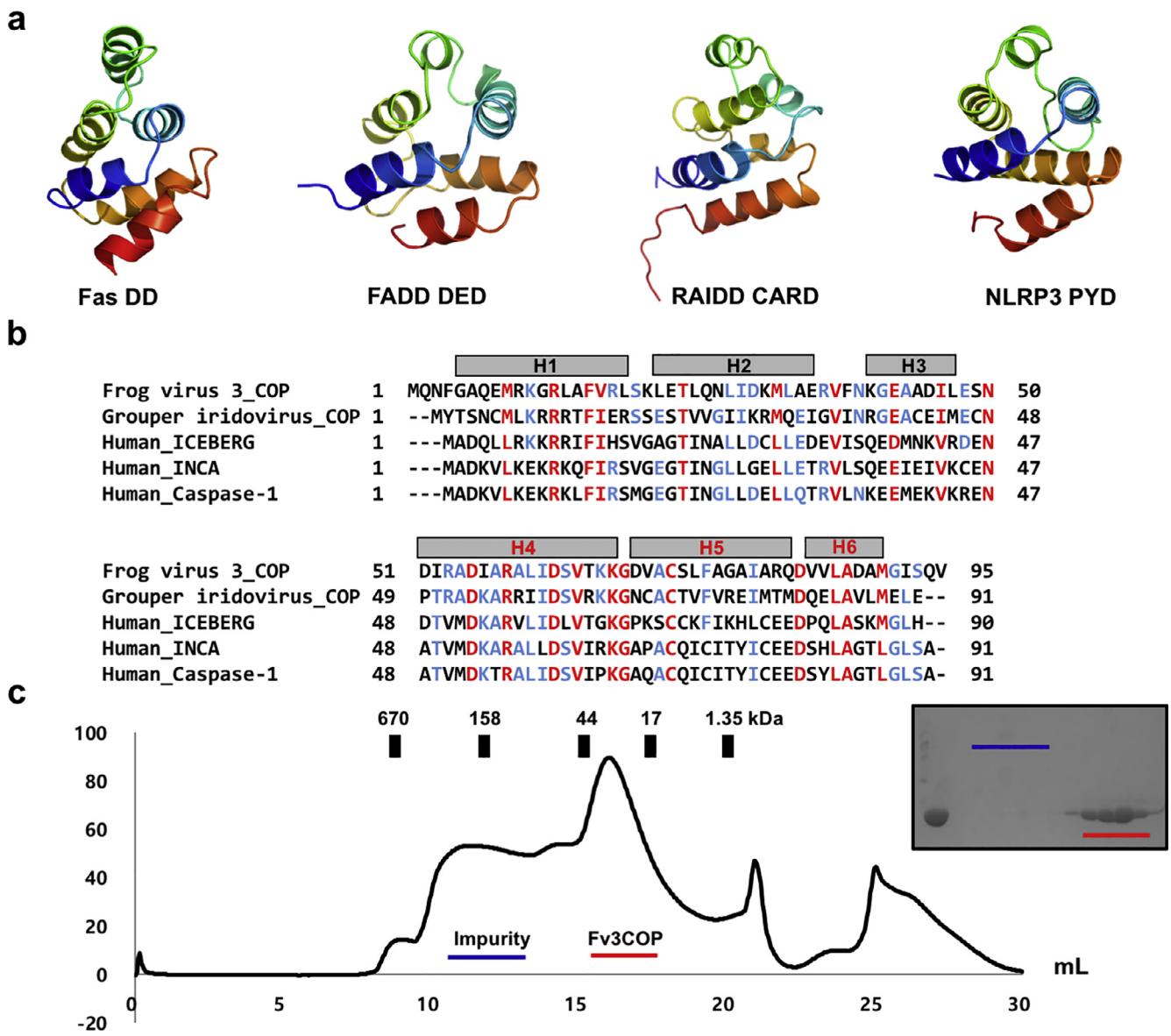

Fig. 1. Identification and purification of Fv3COP. a. Schematic of the structures of DDS subfamily members. Representative structures of each subfamily, including death domain (DD), death effector domain (DED), caspase recruitment domain (CARD), and pyrin domain (PYD), are shown. The structures from the N-terminus (N-term) to the C-terminus (C-term) are colored blue to red. b. Sequence alignment of COPs. Completely/highly-conserved and partially-conserved residues are shown in red and blue, respectively. Secondary structures, H1 to H6, are indicated above the corresponding sequences. The partially unfolded region, from H4 to H6, due to the regional domain-swapping dimerization is shown in red. c. Fv3COP was detected as a dimer in solution. Size-exclusion chromatography profile. The last peak, eluted at around 16–17 mL, was Fv3COP based on SDS-PAGE (indicated by red bar). The other two peaks, which eluted earlier, were impurities (indicated by the blue bar).

been identified as regulators of inflammation and innate immunity (Stehlik and Dorfleutner, 2007; Le and Harton, 2013;4.). These proteins can inhibit the assembly of NOD-like receptor complexes such as the inflammasome and the NODosome, which are critical molecular complexes involved in caspase-1 activation. POPs direct interact with PYD domain in NOD-like receptors or the PYD domain-containing adaptor protein ASC via a PYD-PYD interaction (Le and Harton, 2013;4.; Dorfleutner et al., 2007). COPs are known to interact with either caspase-1 CARD or RIP2 CARD via CARD-CARD interactions (Lee et al., 2001; Humke et al., 2000) and inhibit caspase-1 activation or further downstream signaling. Three are three POPs (POP1, POP2, and POP3) and three COPs (Pseudo-ICE, INCA, and ICEBERG) that have been identified in the human genome (Stehlik and Dorfleutner, 2007; Le and Harton, 2013). It is known that several viruses, including the pox virus, myxoma virus, and the shope fibroma virus, also contain viral POPs that can suppress the host immune response after viral infection (Dorfleutner et al., 2007; Johnston et al., 2005). Although their functions are unclear, sequence analyses have also identified COPs in the genome of certain viruses, including the grouper iridovirus, the soft-shelled turtle iridovirus, and the frog virus (Huang et al., 2009; Tan et al., 2004). To elucidate the molecular mechanism of the inhibition of host immunity by viral COP, we have solved the structure of a viral COP, the CARD-containing protein 064R (UniPortKB: Q6GZR1) from frog virus 3 (hereafter referred to as Fv3COP). Our structure shows that Fv3COP forms a structural transformation-mediated dimer, which is unique and has not been reported in any other structural study of a CARD domain. Recently, novel dimerization processes through structural transformation have been reported in other DDS subfamily members (Scott et al., 2009; Eibl et al., 2014). By comparing our structure with these other cases, we propose that structural transformation-mediated dimerization might be a new strategy for dimer assembly in DDS members.

Table 1
Data collection and refinement statistics.

Data collection	Native
Wavelength	0.9796 Å
Space group	$P2_1$
Cell dimensions	
a, *b*, *c* *α*,*β*,γ	46.65 Å, 60.50 Å, 78.83 Å 90°, 90°, 90°
Resolution	50.0–2.50 Å (2.50–2.54 Å)
Unique reflections	56,672 (15,193)
Wilson B-factor	85.68
I/sigma (*I*)	38.02 (7.86)
Completeness	99.8% (100%)
Redundancy	3.7 (3.6)
R-sym	10.8 (21.6)
R-meas	11.8 (22.3)
Refinement	
Resolution	40.0–2.5 Å
No. reflections used in refinement	15,157
R_{work}/R_{free}	16.8%/23.6%
No. atoms	
Protein	2,851
Water and other small molecules	13
Average B-factors	
Protein	30.6 $Å^2$
Water and other small molecules	25.9 $Å^2$
r.m.s. deviations	
Bond lengths	0.007 Å
Bond angles	0.84°
Ramachandran Plot Most favored regions	98.4% 1.6%
Additional allowed regions	
Rotamer outliers	0.0%
Clashscore	1.7

Statistics for the highest-resolution shell are shown in parentheses.

2. Materials and methods

2.1. Sequence alignment

The amino acid sequences of CARD domains, including Fv3COP, were analyzed using ClustalW2 (http://www.ebi.ac.uk/Tools/msa/clustalw2/).

2.2. Protein expression and purification

Full-length Fv3COP (amino acid residue: 1–95) cloned into pET24a was expressed in *Escherichia coli*. Full-length Fv3COP gene (UniPortKB: Q6GZR1) was amplified by PCR using gene-specific primers containing NdeI and XhoI sites. The PCR fragments were subsequently digested and ligated into the pET24a vector containing a C-terminal *hexa*-histidine tag. The sequences of the cloned genes were verified by DNA sequencing. The resulting plasmid was transformed into BL21 (DE3) *Escherichia coli* competent cells. Following this, the cells were plated onto LB (Luria-Bertani) plates and incubated for 24 h at 37 °C. Next, individual colonies were inoculated into 5 mL of LB media and incubated overnight at 37 °C with shaking. Cultured cells were used to inoculate 1 L of LB media and incubated for 5 h at 37 °C until the O.D. reached 0.78. Protein expression was induced by treating the bacteria with 0.5 mM isopropyl β-D-thiogalactopyranoside (IPTG) for 18 h at 20 °C. Following induction, the bacteria were collected, resuspended, and lysed by sonication in 50 mL of lysis buffer (20 mM Tris-HCl pH 7.9, 500 mM NaCl, 25 mM imidazole). The bacterial lysate was subsequently centrifuged at 10,000 × *g* for 30 min at 4 °C. Following this, the supernatant was applied to a gravity-flow column (Bio-Rad, Hercules, CA, USA) packed with 1.5 mL of Ni-NTA affinity resin (Qiagen, Venlo, Netherlands). The unbound bacterial proteins were subsequently removed from the column using 50 mL of wash buffer (20 mM Tris-HCl pH 7.9, 500 mM NaCl, 60 mM imidazole). The target protein was subsequently eluted from the column using elution buffer (20 mM Tris-HCl pH 8.0, 500 mM NaCl, 250 mM imidazole). Fractions containing more than 90% homogenous protein, assessed by staining of SDS-PAGE gels, were then selected and combined. Protein purity was further improved using a Superdex 200 gel-filtration column 10/30 (GE Healthcare, Waukesha, WI, USA) pre-equilibrated with a solution of 20 mM Tris-HCl pH 8.0 and 150 mM NaCl. Peak fractions were collected, pooled, and concentrated to 5.3 mg/mL for crystallization.

2.3. Crystallization and data collection

Crystallization of Fv3COP was conducted at 20 °C by the hanging drop vapor-diffusion method using a crystallization screening kit from Hampton Research (Laguna Niguel, CA, USA). The initial crystal was grown on plates by equilibrating a mixture containing 1 μL of protein solution (5.3 mg/mL protein in 20 mM Tris pH 8.0 and 150 mM NaCl) and 1 μL of reservoir solution containing 2.5 M NaCl and 0.1 M imidazole pH 8.0 against 0.3 mL of reservoir solution. The best crystal used for the structural study was produced by adding 10% w/v PEG 3350 to the reservoir solution. The crystal grew to maximum dimensions of 0.1 × 0.1 × 0.01 mm in three days. A 2.5 Å dataset was collected at the SB-II (5C) beamline at Pohang Accelerator Laboratory (PAL), Republic of Korea. Data processing and scaling was carried out using HKL2000 (Minor et al., 2006)

2.4. Structure determination and analysis

The molecular replacement (MR) phasing method was conducted with Phaser (McCoy, 2007). The human ICEBERG structure was used as the search model (PDBid: 1DGN) (Humke et al., 2000). The initial solution model was extended and completed by iterative manual building and refinement using Coot (Emsley and Cowtan, 2004) and PHENIX Refine (Adams et al., 2010), respectively. The quality of the model was checked using PROCHECK (Laskowski et al., 1993;26.). Molecular structural images were generated using the PyMOL Molecular Graphics System, Version 1.3 Schrödinger, LLC (DeLano and Lam, 2005).

2.5. Protein data bank accession codes

The coordinate and structural factor were deposited in the Protein Data Bank under PDB ID code: 6J52.

3. Results

3.1. Frog virus 3 contains COP, which dimerizes in solution

The CARD domain is a protein interaction module belonging to the death domain superfamily (DDS), which includes the death domain (DD), the death effector domain (DED), and the Pyrin domain (PYD). The structure of the Fas DD, a DDS member, was first reported using nuclear magnetic resonance (NMR) (Tartaglia et al., 1993) followed by FADD (Fas-associated death domain protein), DED (Chinnaiyan et al., 1995), RAIDD (RIP-associated protein with a death domain), CARD (Chou et al., 1998), and NLRP3 (NACHT, leucine-rich repeat and PYD containing 3) PYD (Bae and Park, 2011). The representative structure for each subfamily revealed a six-helix bundle fold as being the common DDS structural feature (Fig. 1a).

Virus-infected host cells use apoptosis as a primary defense mechanism to prevent viral spread. However, several viruses have evolved strategies that can counteract this host defense mechanism. Viral-FLIP and viral Bcl-2 homologs are proteins that can be used to disrupt apoptosis in the host cell after viral infection. In this regard, viruses also express PYD-only proteins (vPOP), such as M013, to escape the host defense system. Although the viral CARD-only protein (vCOP) has not been well characterized, a recent study showed that grouper iridoviruses contains vCOP, and that this protein inhibits host apoptosis signaling by inhibiting both caspase-8 and -9 (Chen et al., 2015). A

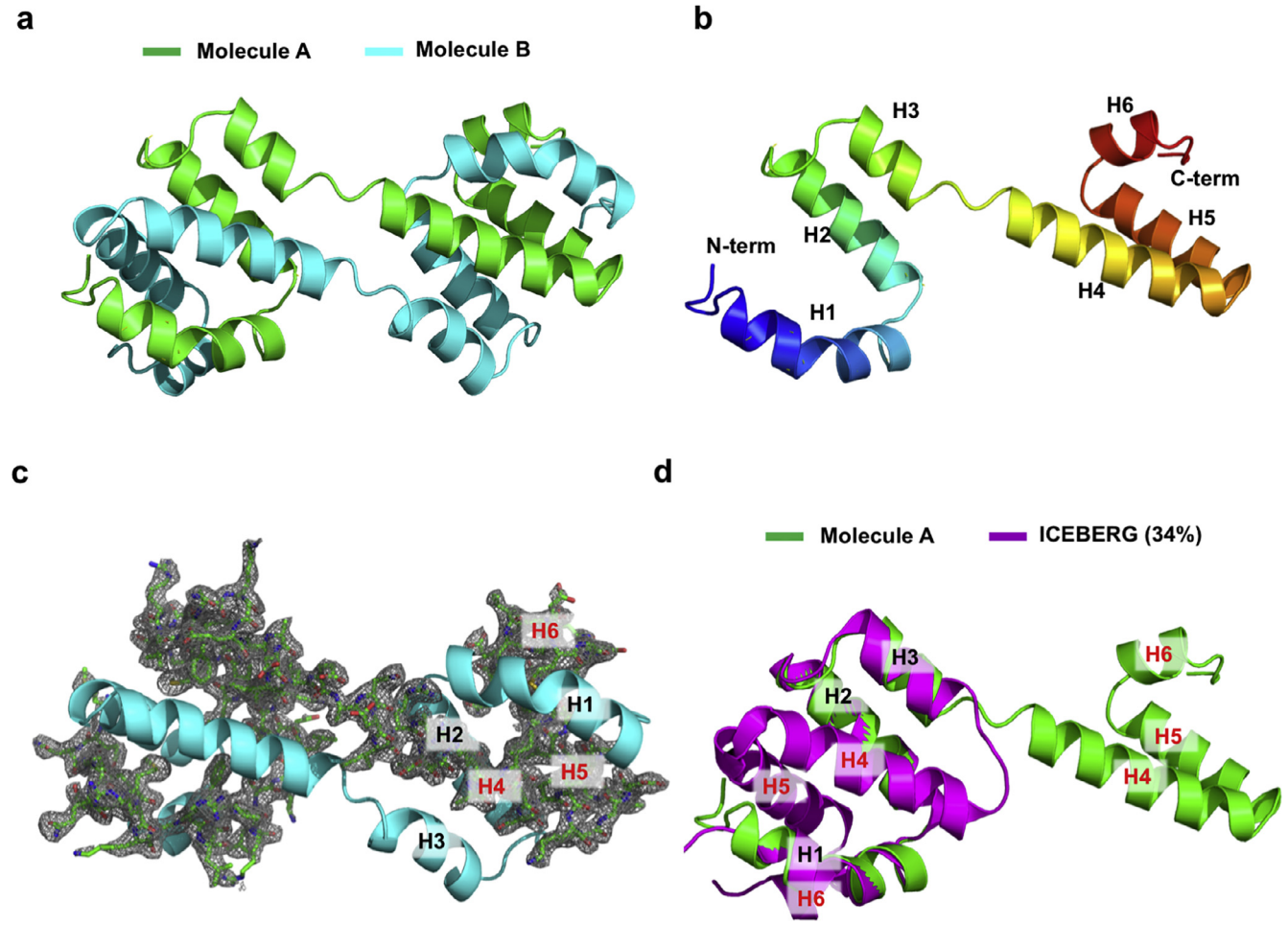

Fig. 2. Structure of Fv3COP. a. Structure of Fv3COP dimer b. Structure of Fv3COP monomer. Secondary structures, from H1 to H6, are shown on the corresponding helixes. The structure from the N-terminus (N-term) to the C-terminus (C-term) is colored blue to red. c. A 2Fo-Fc density map contoured at the 1-σ level around molecule A. Helixes H1 to H3 are colored black and are from molecule B, while helixes H4 to H6 are colored red and are from molecule A. d. Structural comparison of extended Fv3COP (green color) with its structural homologue ICEBERG (magenta color), human COP.

sequence similarity search showed that several virus genomes, including frog virus 3, also contains vCOP (Fv3COP) (Fig. 1b). The sequence identity between Fv3COP and human COPs (ICEBERG and INCA) is around 30%. We purified Fv3COP and crystallized it to perform the first structural study of a vCOP in order to reveal how vCOPs can inhibit host defense mechanisms. Size-exclusion chromatography (SEC) showed that Fv3COP formed a dimer in solution, with an elution volume of around 16 mL from the SEC-column (Fig. 1c).

3.2. Structure of Fv3COP

To elucidate the mechanism by which vCOP functions as part of a host-defense escape mechanism, we determined the first crystal structure of vCOP at 2.5 Å resolution. The structure of human COP, ICEBERG (PDBid: 1DGN) (Humke et al., 2000), has been solved, and since this domain shares around a 30% sequence identity with vCOP it was used as a search model for molecular replacement (MR). The structure was refined to a R_{work} = 16.8% and R_{free} = 23.6%. The data collection and refinement statistics are summarized in Table 1. Four molecules, two dimers, were located in the asymmetric unit. During the model building step, we realized that two molecules form dimers by exchanging a part of the molecule, which is partially unfolded and extended in the opposite direction (Fig. 2a). The high-resolution structure of Fv3CARD monomer revealed that it comprised six helices, H1–H6 (Fig. 2b). However, the structure was not a typical six-helical bundle fold found in DDS family members. H4, H5, and H6 in Fv3COP were completely unfolded and extended in an opposite direction (Fig. 2b). Because previous biochemical and structural studies showed that CARD domains can exist as monomers, dimers, or even higher oligomeric forms in solution without structural changes (Jang et al., 2015; Jang et al., 2013; Peisley et al., 2014; Xu et al., 2014), helix-exchange mediated dimerization might be an alternative method for CARD-dimerization. The electron density clearly showed that the helix bundle fold of the Fv3COP was partially unfolded and was used for domain swapping (Fig. 2c). When compared to the monomeric structure of the human COP, ICEBERG, displacement of the helix bundle folds was found from H4 to H6 (Fig. 2d). For domain swapping, the displaced H4, H5, and H6 bundle folds in molecule A are inserted into a second molecule (molecule B) to form a complete six helix bundle fold consisting of H1, H2, and H3 from molecule B and H4, H5, and H6 from molecule A, providing a structure which is typical for the death domain superfamily, including CARD (Fig. 2c and d).

3.3. Analysis of dimer interface

Fv3COP dimerizes through regional domain-swapping. A surface representation showed that extended Fv3COP fitted well into the surface cleft formed by another, opposite, extended Fv3COP molecule (Fig. 3a). The interface was formed by a large number of H-bonds and salt bridges, which buried ~3237 $Å^2$ of the total accessible surface area of 8390 $Å^2$ (Fig. 3b and c). A PISA interface analyzing server gave a complex formation significance score (CSS) of 1.000 in indicating that

a

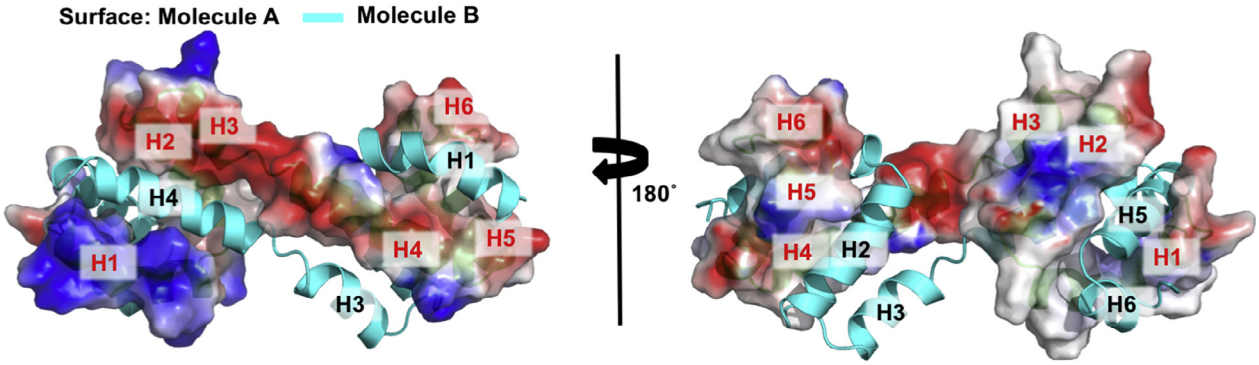

b

Molecule B	Molecule A	Distance(A)
Q2	S93	2.67
F4	S73	2.96
R13	D62	3.05
N27	Q82	2.73
R53	S20	2.93
K67	E42	2.71
S73	F4	3.16
S93	Q2	3.7

c

Molecule B	Molecule A	Distance(A)
R13	D62	3.05
K21	D83	3.30
K67	E42	2.71
D62	R13	2.85
E42	K67	2.69

Fig. 3. The interface of the regional domain-swapped dimer of Fv3COP. a Representation of the electrostatic surface of Fv3CO showing the interface of the domain-swapped dimer. b and c. Tables showing specific residues that participate in H-bond formation (b) and salt bridge formation (c).

the regional domain-swapped dimer was the optimal form found in solution. For stable dimer formation, the H4, H5, and H6 helix bundles displaced by regional domain-swapping were inserted in between H1, H2, and H3 of an opposite molecule, wrapping and forming the typical six helix bundle fold found in DDS family members. In addition to hydrophobic interactions and hydrogen bonds, massive salt bridges were formed through regional domain-swapping. R13, E42, D62, K67, and D83 from molecule A formed salt bridges with R13, K21, E42, D62, and K67 from the opposite molecule B (Fig. 3c). This combination of interactions made the dimeric complex stable.

3.4. Structural transformation-mediated dimerization might be a common strategy for dimer assembly in DDS

DDS dimerization arising as a result of the structural transformation arising through the open-closed state interchange revealed in this study (Fig. 4a) and has been previously described in structural studies of other DDS subfamily members. The first example was reported in 2009 from a structural study of the Fas DD/FADD DD complex involved in the assembly of the death inducing signaling complex (DISC) (Scott et al., 2009). In this study, the idea of a structural transformation of DD was introduced for the first time. Here, H5 and H6 interacted with one another, forming a single helix referred to as a stem helix (Fig. 4b). Fas DD dimerization, mediated by this stem helix, is critical for the binding of FAS DD to FADD DD, a binding partner that is critical for DISC assembly. A closed-inactive (a typical six-helix bundle fold) and an open-active conformation (a stem helix formed by the interaction of H5-H6) in DD have been suggested to be important regulators of DISC mediated caspase-8 activation in the extrinsic apoptosis pathway. Structural transformation-mediated dimerization of the PYD subfamily was also shown in a structural study of NLRP14 PYD (Eibl et al., 2014). Similar to the case for the Fas DD, NLRP14 PYD showed an interaction between H5-H6, resulting in an extended stem helix at the C-terminus (Fig. 4c). This structural transformation resulted in an extended stem helix that mediates a novel symmetric pyrin-domain dimerization (Fig. 4c). A novel domain-swapping strategy for DED dimerization was most recently highlighted in a report of the structure of tandem DEDs in caspase-8, which showed that the FL motif in DED2, but not in DED1, is critical for dimerization and further activation of caspase-8 in DISC. In this structure, DED1 was intact, but DED2 had undergone a structural transformation. The displacement of the helix bundle fold started from H3 to H6 of DED2. For domain swapping, the displaced H4, H5, and H6 helix bindles in molecule A are inserted into another molecule (molecule B) in order to interact with its H1, H2 and H3 helix bundles and form a complete six helix bundle fold (Fig. 4d).

4. Discussion

In humans, several CARD-only proteins (COPs), such as ICEBERG and INCA, have been identified and are known to regulate the activity of caspases by inhibiting the formation of the caspase-activating complex through CARD-CARD interaction. COPs are found in several viruses including frog virus 3. Although a recent study showed that viral COP (vCOP) inhibits both intrinsic and extrinsic apoptosis signaling by reducing the activity of caspases, a clear mechanism of how vCOPs function has not yet been reported (Chen et al., 2015). Because viruses have evolved to escape host defense by expressing both anti-apoptotic and anti-immunity molecules, vCOP has also been suggested to be an anti-host defense molecule (Chen et al., 2015). In order to understand the mechanism by which vCOPs regulates both intrinsic and

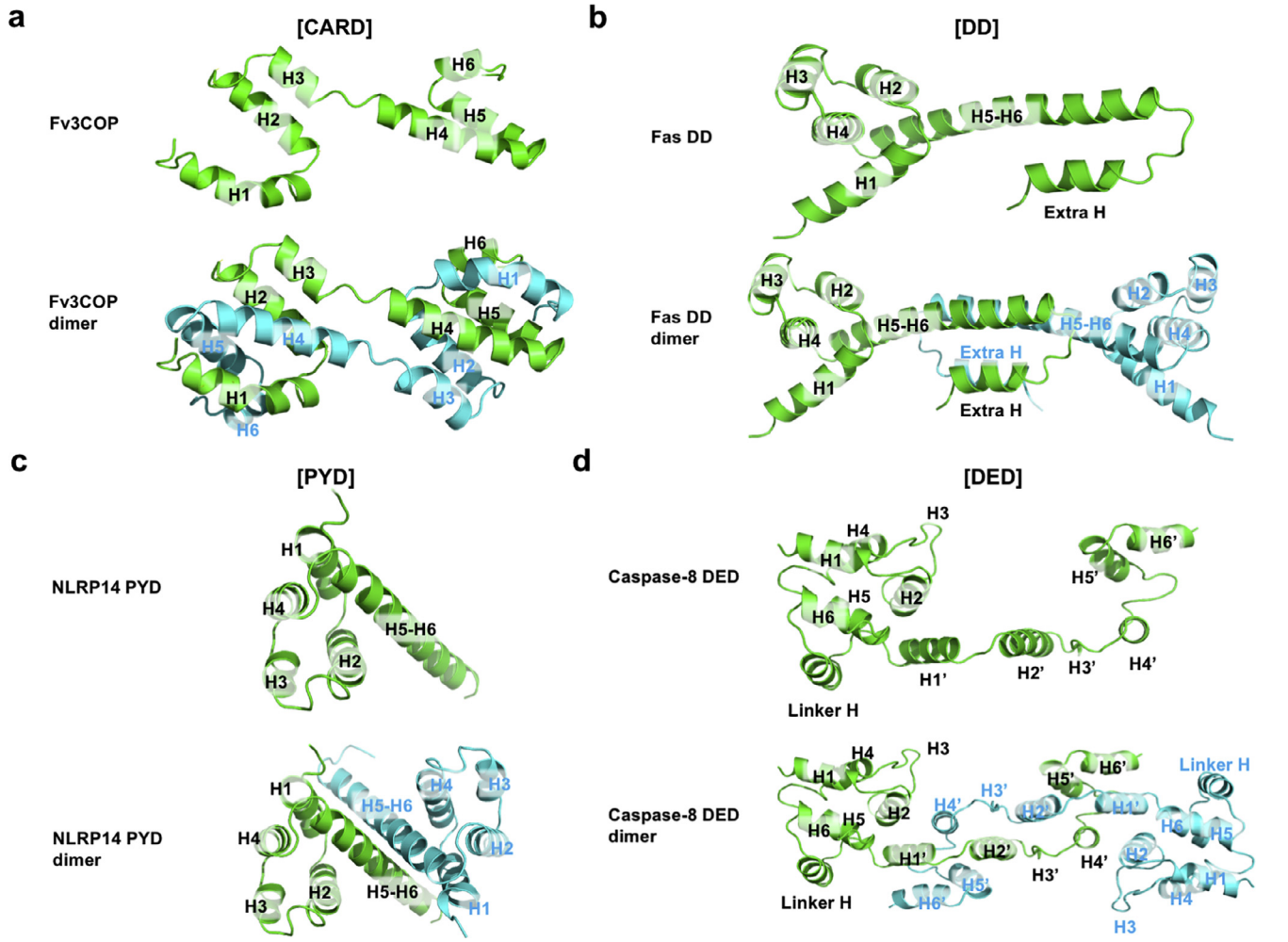

Fig. 4. Domain-swapped dimers of the death domain superfamily. a. Structure of the domain-swapped dimer of the CARD subfamily. A monomer (upper panel) and a dimer (lower panel) of Fv3COP are shown as cartoon figures. Each helix is labelled on the corresponding helix. b. Structure of the domain-swapped dimer of the DD subfamily. A monomer (upper panel) and a dimer (lower panel) of Fas DD are shown as cartoon figures. c. Structure of the domain-swapped dimer of the PYD subfamily. A monomer (upper panel) and a dimer (lower panel) of Fas DD are shown as cartoon figures. d. Structure of the domain-swapped dimer of the caspase-8 tandem DEDs. A monomer (upper panel) and a dimer (lower panel) of Fas DD are shown as cartoon figures.

extrinsic apoptosis, as well as innate immunity, we determined the structure of COP from the frog virus 3 (Fv3COP).

The structure showed that Fv3COP dimerized via structural transformation-mediated domain swapping, which is the first case of CARD domain. Helix bundles H4, H5, and H6 from one molecule in the dimer were unfolded, displaced and extended to the opposite molecule. The re-located H4, H5, and H6 helix bundles form a complete six-helix bundle fold with the H1, H2, and H3 helix bundle from the opposite molecule. Although the translocation regions were not identical, a similar domain swapping-mediated dimerization has been found from structural studies of other DDS subfamily members. In the case of DD and PYD, helix bundles H5 and H6 connect with each other to form a stem helix, which mediates the dimerization of DDs and PYDs (Scott et al., 2009; Eibl et al., 2014). Domain-swapping mediated dimerization of DED was also reported in the structure of caspase-8 tandem DEDs (Park, 2018), where DED2-mediated domain swapping was observed. The displacement of the helix bundle folds was found in H3–H6 of DED2. For domain swapping, the displaced H4, H5, and H6 helix bindles in molecule A are inserted into another molecule (molecule B) in order to interact with its H1, H2, and H3 helix bundles and form a complete six helix bundle fold.

Although structural transformation-mediated dimerization (or domain-swapped dimer) has been reported for several DDS members, whether this dimerization is artificial is still a question. In the case of structural studies of Fas-FADD DD complex (Wang et al., 2010) and caspase-8 tandem DEDs (Shen et al., 2015; Fu et al., 2016), they are formed helical oligomer without structural alterations. These previous studies indicated that the canonical six-helix bundle forms are capable of oligomerization as well. Because DDS-containing proteins can form many different oligomeric complexes with various signaling molecules during apoptosis, necroptosis, and other immune signaling pathways, by acting as enzymes and sometimes scaffolding adaptors (Chun et al., 2002; Wang et al., 2008), it is not surprising that several different modes of oligomerization, including structural transformation-mediated regional domain-swapping dimer formation, and the previously reported helical oligomer (Lu et al., 2014; Peisley et al., 2014; Fu et al., 2016; Choi et al., 2017), can be found in cells. Taken together, structural transformation-mediated dimerization might be a common strategy for dimer assembly in DDS members.

Acknowledgments

This study was supported by the Basic Science Research Program through the National Research Foundation of Korea (NRF) of the Ministry of Education, Science, and Technology (NRF-2017M3A9D8062960 and NRF-2018R1A2B2003635), and a grant from Korea Polar Research Institute (grant number PE19210).

References

Park, H.H., Lo, Y.C., Lin, S.C., Wang, L., Yang, J.K., Wu, H., 2007. The death domain superfamily in intracellular signaling of apoptosis and inflammation. Ann. Rev. Immunol. 25, 561–586.

Kwon, D., Yoon, J.H., Shin, S.Y., Jang, T.H., Kim, H.G., So, I., et al., 2012. A comprehensive manually curated protein-protein interaction database for the Death Domain superfamily. Nucleic Acids Res. 40, D331–D336.

Acehan, D., Jiang, X., Morgan, D.G., Heuser, J.E., Wang, X., Akey, C.W., 2002. Three-dimensional structure of the apoptosome: implications for assembly, procaspase-9 binding, and activation. Mol. Cell 9, 423–432.

Park, H.H., Logette, E., Rauser, S., Cuenin, S., Walz, T., Tschopp, J., et al., 2007. Death domain assembly mechanism revealed by crystal structure of the oligomeric PIDDosome core complex. Cell 128, 533–546.

Dickens, L.S., Boyd, R.S., Jukes-Jones, R., Hughes, M.A., Robinson, G.L., Fairall, L., et al., 2012. A death effector domain chain DISC model reveals a crucial role for caspase-8 chain assembly in mediating apoptotic cell death. Mol. Cell 47, 291–305.

Lu, A., Magupalli, V.G., Ruan, J., Yin, Q., Atianand, M.K., Vos, M.R., et al., 2014. Unified polymerization mechanism for the assembly of ASC-dependent inflammasomes. Cell 156, 1193–1206.

Hornung, V., Ablasser, A., Charrel-Dennis, M., Bauernfeind, F., Horvath, G., Caffrey, D.R., et al., 2009. AIM2 recognizes cytosolic dsDNA and forms a caspase-1-activating inflammasome with ASC. Nature 458, 514–518.

Stanger, B.Z., Leder, P., Lee, T., Kim, E., Seed, B., 1995. RIP: a novel protein containing a death domain that interacts with Fas/APO-1 (CD95) in yeast and causes cell death. Cell 81, 513–523.

Golstein, P., Marguet, D., Depraetere, V., 1995. Homology between reaper and the cell death domains of Fas and TNFR1. Cell 81, 185–186.

Akira, S., Uematsu, S., Takeuchi, O., 2006. Pathogen recognition and innate immunity. Cell 124, 783–801.

Pichlmair, A., Schulz, O., Tan, C.P., Naslund, T.I., Liljestrom, P., Weber, F., et al., 2006. RIG-I-mediated antiviral responses to single-stranded RNA bearing 5'-phosphates. Science 314, 997–1001.

Sukits, S.F., Lin, L.L., Hsu, S., Malakian, K., Powers, R., Xu, G.Y., 2001. Solution structure of the tumor necrosis factor receptor-1 death domain. J. Mol. Biol. 310, 895–906.

Tsao, D.H., McDonagh, T., Telliez, J.B., Hsu, S., Malakian, K., Xu, G.Y., et al., 2000. Solution structure of N-TRADD and characterization of the interaction of N-TRADD and C-TRAF2, a key step in the TNFR1 signaling pathway. Mol. Cell 5, 1051–1057.

Yang, J.K., Wang, L., Zheng, L., Wan, F., Ahmed, M., Lenardo, M.J., et al., 2005. Crystal structure of MC159 reveals molecular mechanism of DISC assembly and FLIP inhibition. Mol. Cell 20, 939–949.

Bae, J.Y., Park, H.H., 2011. Crystal structure of NALP3 protein pyrin domain (PYD) and its implications in inflammasome assembly. J. Biol. Chem. 286, 39528–39536.

Hofmann, K., Bucher, P., Tschopp, J., 1997. The CARD domain: a new apoptotic signalling motif. Trends Biochem. Sci. 22, 155–156.

Stehlik, C., Dorfleutner, A., 2007. COPs and POPs: modulators of inflammasome activity. J. Immunol. 179, 7993–7998.

Le, H.T., Harton, J.A., 2013.. Pyrin- and CARD-only proteins as regulators of NLR functions. Front. Immunol. 4.

Dorfleutner, A., Bryan, N.B., Talbott, S.J., Funya, K.N., Rellick, S.L., Reed, J.C., et al., 2007. Cellular pyrin domain-only protein 2 is a candidate regulator of inflammasome activation. Infect. Immun. 75, 1484–1492.

Lee, S.H., Stehlik, C., Reed, J.C., 2001. Cop, a caspase recruitment domain-containing protein and inhibitor of caspase-1 activation processing. J. Biol. Chem. 276, 34495–34500.

Humke, E.W., Shriver, S.K., Starovasnik, M.A., Fairbrother, W.J., Dixit, V.M., 2000. ICEBERG: a novel inhibitor of interleukin-1beta generation. Cell 103, 99–111.

Dorfleutner, A., Talbott, S.J., Bryan, N.B., Funya, K.N., Rellick, S.L., Reed, J.C., et al., 2007. A shope fibroma virus PYRIN-only protein modulates the host immune response. Virus Genes 35, 685–694.

Johnston, J.B., Barrett, J.W., Nazarian, S.H., Goodwin, M., Ricciuto, D., Wang, G., et al., 2005. A poxvirus-encoded pyrin domain protein interacts with ASC-1 to inhibit host inflammatory and apoptotic responses to infection. Immunity 23, 587–598.

Huang, Y., Huang, X., Liu, H., Gong, J., Ouyang, Z., Cui, H., et al., 2009. Complete sequence determination of a novel reptile iridovirus isolated from soft-shelled turtle and evolutionary analysis of Iridoviridae. BMC Genomics 10, 224.

Tan, W.G., Barkman, T.J., Gregory Chinchar, V., Essani, K., 2004. Comparative genomic analyses of frog virus 3, type species of the genus Ranavirus (family Iridoviridae). Virology 323, 70–84.

Scott, F.L., Stec, B., Pop, C., Dobaczewska, M.K., Lee, J.J., Monosov, E., et al., 2009. The Fas-FADD death domain complex structure unravels signalling by receptor clustering. Nature 457, 1019–1022.

Eibl, C., Hessenberger, M., Wenger, J., Brandstetter, H., 2014. Structures of the NLRP14 pyrin domain reveal a conformational switch mechanism regulating its molecular interactions. Acta Crystallogr. Sect. D Biol. Crystallogr. 70, 2007–2018.

Minor, W., Cymborowski, M., Otwinowski, Z., Chruszcz, M., 2006. HKL-3000: the integration of data reduction and structure solution-from diffraction images to an initial model in minutes. Acta Crystallogr. Sect. D Biol. Crystallogr. 62, 859–866.

McCoy, A.J., 2007. Solving structures of protein complexes by molecular replacement with Phaser. Acta Crystallogr. Sect. D Biol. Crystallogr. 63, 32–41.

Emsley, P., Cowtan, K., 2004. Coot: model-building tools for molecular graphics. Acta Crystallogr. Sect. D Biol. Crystallogr. 60, 2126–2132.

Adams, P.D., Afonine, P.V., Bunkoczi, G., Chen, V.B., Davis, I.W., Echols, N., et al., 2010. PHENIX: a comprehensive Python-based system for macromolecular structure solution. Acta Crystallogr. Sect. D Biol. Crystallogr. 66, 213–221.

Laskowski, R.A., MacArthur, M.W., Moss, D.S., Thornton, J.M., 1993.. PROCHECK: a program to check the stereochemical quality of protein structures. J. Appl. Cryst. 26.

DeLano, W.L., Lam, J.W., 2005. PyMOL: A communications tool for computational models. Abstr Pap Am Chem S. 230, U1371–U1372.

Tartaglia, L.A., Ayres, T.M., Wong, G.H., Goeddel, D.V., 1993. A novel domain within the 55 kd TNF receptor signals cell death. Cell 74, 845–853.

Chinnaiyan, A.M., O'Rourke, K., Tewari, M., Dixit, V.M., 1995. FADD, a novel death domain-containing protein, interacts with the death domain of Fas and initiates apoptosis. Cell 81, 505–512.

Chou, J.J., Matsuo, H., Duan, H., Wagner, G., 1998. Solution structure of the RAIDD CARD and model for CARD/CARD interaction in caspase-2 and caspase-9 recruitment. Cell 94, 171–180.

Chen, C.W., Wu, M.S., Huang, Y.J., Lin, P.W., Shih, C.J., Lin, F.P., et al., 2015. Iridovirus CARD Protein Inhibits Apoptosis through Intrinsic and Extrinsic Pathways. PLoS One 10, e0129071.

Jang, T.H., Kim, S.H., Jeong, J.H., Kim, S., Kim, Y.G., Park, H.H., 2015. Crystal structure of caspase recruiting domain (CARD) of apoptosis repressor with CARD (ARC) and its implication in inhibition of apoptosis. Sci. Rep. 5, 9847.

Jang, T.H., Park, J.H., Park, H.H., 2013. Novel disulfide bond-mediated dimerization of the CARD domain was revealed by the crystal structure of CARMA1 CARD. PLoS One 8, e79778.

Peisley, A., Wu, B., Xu, H., Chen, Z.J., Hur, S., 2014. Structural basis for ubiquitin-mediated antiviral signal activation by RIG-I. Nature 509, 110–114.

Xu, H., He, X., Zheng, H., Huang, L.J., Hou, F., Yu, Z., et al., 2014. Structural basis for the prion-like MAVS filaments in antiviral innate immunity. eLife 3, e01489.

Park, H.H., 2018. Molecular basis of dimerization of initiator caspase was revealed by crystal structure of caspase-8 pro-domain. Cell Death Differ.

Wang, L., Yang, J.K., Kabaleeswaran, V., Rice, A.J., Cruz, A.C., Park, A.Y., et al., 2010. The Fas-FADD death domain complex structure reveals the basis of DISC assembly and disease mutations. Nat. Struct. Mol. Biol. 17, 1324–1329.

Shen, C., Yue, H., Pei, J., Guo, X., Wang, T., Quan, J.M., 2015. Crystal structure of the death effector domains of caspase-8. Biochem. Biophys. Res. Commun. 463, 297–302.

Fu, T.M., Li, Y., Lu, A., Li, Z., Vajjhala, P.R., Cruz, A.C., et al., 2016. Cryo-EM structure of caspase-8 tandem DED filament reveals assembly and regulation mechanisms of the death-inducing signaling complex. Mol. Cell 64, 236–250.

Chun, H.J., Zheng, L., Ahmad, M., Wang, J., Speirs, C.K., Siegel, R.M., et al., 2002. Pleiotropic defects in lymphocyte activation caused by caspase-8 mutations lead to human immunodeficiency. Nature 419, 395–399.

Wang, L., Du, F., Wang, X., 2008. TNF-alpha induces two distinct caspase-8 activation pathways. Cell 133, 693–703.

Choi, J.Y., Qiao, Q., Hong, S.H., Kim, C.M., Jeong, J.H., Kim, Y.G., et al., 2017. CIDE domains form functionally important higher-order assemblies for DNA fragmentation. Proc. Natl. Acad. Sci. U.S.A. 114, 7361–7366.